

Ground-state correlations and linear response of metal clusters

C. Yannouleas

School of Physics, Georgia Institute of Technology, Atlanta, Georgia 30332-0430

F. Catara

Dipartimento di Fisica and Istituto Nazionale di Fisica Nucleare, Sezione di Catania, I-95129 Catania, Italy

N. Van Giai

Division de Physique Théorique, Institut de Physique Nucléaire, F-91406 Orsay Cedex, France

(Received 11 August 1994; revised manuscript received 12 October 1994)

The composition of the random-phase-approximation ground state in metal clusters is explicitly determined. It is shown that, due to the long-range character of the Coulomb interaction, multi-configurational, higher-order correlations in the ground state play a more important role than had been previously assumed. However, the deviations between single-particle occupation probabilities associated with the correlated ground state and the uncorrelated reference determinant are found to be small, thus validating the quasiboson approximation. The reliability of various many-body approaches in describing excited collective modes depends crucially on their ability of adequately approximating these correlations in the composition of the ground-state wave function. In this context, the consistency of random-phase-approximation and configuration-interaction results in metal clusters is assessed through a comparison with established experimental trends and known theoretical limits of the exact many-body problem.

I. INTRODUCTION

In the past few years, the photoabsorption of metal clusters has been extensively studied using the matrix random-phase approximation (matrix RPA) upon a jellium background¹⁻⁵ [with a two-body interaction derived from the local-density approximation (LDA)]. This method provides a unifying framework for describing the evolution of the optical response both as a function of size^{4,5} and as a function of the excess positive or negative charge.^{1,3} In particular, we note that the calculated sizes cover a broad range, from the rather small (e.g., Na₈) to the very large (e.g., Na₁₉₈₂). The method has also been utilized for describing the collective excitations in He₃ clusters⁶ (without a jellium-background approximation), and has been extended to the study of two-boson and nonlinear effects in metal clusters.⁷

A related, but mathematically different formulation of linear response, known as time-dependent LDA (TDLDA), has also been widely used for describing the optical properties of metal clusters.⁸⁻¹⁰ The two methods have produced results that are in basic agreement with each other.

Recently, Koskinen *et al.*¹¹ have calculated the photoabsorption of the three smallest magic sodium clusters Na₂, Na₈, and Na₂₀, using a different approach, namely, a configuration-interaction (CI) method upon a jellium background. Unlike the RPA method, which by construction seeks an appropriate linear-response approximation of the equations of motion governing the excited collective vibrations, conceptually the CI method has no limitations *a priori* and may be viewed, in principle, as

seeking an exact solution of the many-body problem by diagonalizing the many-body Hamiltonian in the complete $0p-0h$, $1p-1h$, $2p-2h$, ..., $np-nh$, ... space. In practice, however, this latter method is limited by the numerical power of the available computers, and as a result, the largest possible subspace of order n (the so-called *best* space) is used instead of the complete space. The success of the method depends on whether convergence can be reached within this restricted best space.

Certainly, since the CI appears at first glance to be a complete approach, its successful application promises substantial insights concerning the validity of other, *a priori* approximate approaches. Furthermore, since it is natural to expect that the method will yield better results the smaller the system under consideration, metal clusters appear as fertile ground for its application. In this respect, it is important to reevaluate the results of Ref. 11, to highlight the actual practical and numerical limitations of the CI method regarding jellium spheres, and to answer certain tentative criticisms¹¹ of the matrix RPA, which arose from the discrepancies between CI and RPA results for the optical spectra of sodium clusters.

In the present paper, we intend to assess the consistency of both RPA and CI results by contrasting them (i) against established experimental trends, such as the lowering of the plasmon energy below the classical Mie resonance in the case of smaller clusters;^{12,13} (ii) against known theoretical limits of the exact problem, such as the convergence of the plasmon towards the classical Mie value in the case of both the very large neutral clusters^{14,15} and the highly charged cations;^{16,17,13,11} (iii) against the extent of satisfying the sum rules that are an

integral part of the properties of photoabsorption cross sections.^{18,19}

As will be explicitly discussed below, the matrix RPA satisfies all three consistency requirements mentioned above to a substantially higher degree than the CI method. This in turn raises a further question at a more fundamental many-body level, namely, which basic many-body property of the finite electron gas does the RPA approximate so well that it provides the best description for the collective excitations of metal clusters? To answer this question, we will study the correlations in the RPA ground state, and we will stress the fact that it comprises correlations of all $2np-2nh$ orders.²⁰⁻²⁷ More importantly, we will explicitly show that the RPA ground-state correlations exhibit a unique behavior where higher-order contributions play a more important role than had been previously presumed with regard to metal clusters.^{19,11} In this context, we will show that the proposal for a CI “analog” (which according to Ref. 11 can be constructed by restricting the CI diagonalization to subspaces comprising only $2p-2h$ correlations in the ground state) of an RPA plasmon is based on an underestimation of the importance of higher-order correlations in the ground state.

Furthermore, we note that the importance of correlations in the RPA ground state is intricately related to the role played by the backward-going RPA Y amplitudes entering into the equations of motion. Indeed, from a technical point of view these amplitudes are used to determine the composition of the RPA ground state (and not *vice versa*), and thus it is apparent that they implicitly reflect the influence of the ground-state correlations on the plasmon properties, like position and oscillator-strength distribution. Finally, we show that the underlying physical reason for the large Y amplitudes (large in relative terms with respect to the forward-going X amplitudes), and thus for the strong ground-state correlations in metal clusters, is the long-range character of the Coulomb interaction, a situation which is quite dissimilar from the case of nuclei.

II. CONSISTENCY REQUIREMENTS

A. The limit of large neutral sodium clusters

We note here that according to Ref. 11, large Na_N clusters with $N > 20$ cannot be reached with the CI method, because of excessive lack of convergence, much stronger than the lack of convergence in smaller sizes which Koskinen *et al.* were willing to accept. On the contrary, matrix-RPA calculations have been reported for the full series of magic clusters from Na_8 to Na_{338} ,⁴ and in one instance even for Na_{1982} .⁵

The CI calculation for Na_{20} inside the best space¹¹ could not reproduce the double-peak structure characteristic of the matrix RPA¹ and TDLDA⁸⁻¹⁰ approaches. This should not be surprising, since admittedly¹¹ the CI calculation had not converged. Unexpectedly, however, Koskinen *et al.* concluded from this discrepancy that the RPA method, rather than the CI approach, may be

unreliable for large jellium clusters.

The conclusion of Ref. 11 notwithstanding, we demonstrate here the reliability of the matrix-RPA calculations through a direct confrontation with the classical prediction of the Mie theory¹⁴ for large clusters. According to the Mie theory, a spherical metallic particle (large cluster) absorbs light at a frequency ω_{Mie} , such that $\epsilon(\omega_{\text{Mie}}) = -2$, where $\epsilon(\omega)$ is the bulk dielectric constant of the metal. If the metal can be considered as a free-electron gas, the bulk dielectric constant is given by the Drude approximation [namely, $\epsilon(\omega) = 1 - (\omega_{\text{pla}}/\omega)^2$], and thus the Mie energy is equal to $\hbar\omega_{\text{Mie}} = \hbar\omega_{\text{pla}}/\sqrt{3}$, where the frequency of the volume plasmon is given by $\omega_{\text{pla}} = \sqrt{4\pi e^2 \rho/m_e}$ (ρ denotes the jellium density).

As long as the free-electron mass m_e is not replaced by an effective mass,^{4,28} the matrix RPA must go over to this Drude-Mie limit in the case of very large clusters. Figure 1, which displays the RPA response for Na_{952} , shows that the matrix RPA conforms to a high degree to this limit. Indeed the oscillator strength consists of a band of lines concentrated in a narrow region slightly below 3.4 eV (this value is equal to the Mie energy for a Wigner-Seitz radius $r_s = 4.0$ a.u., appropriate for sodium).

Since $N = 952$ is sufficiently large, the average position of these lines can be found from the relation $\hbar\omega = 3.4/\sqrt{\alpha_0}$ eV, where α_0 is the static polarizability in units of R^3 ($R = r_s N^{1/3}$ is the radius of the positive jellium background). For Na_{952} , the matrix-RPA calculation yielded $\alpha_0 = 1.07$, and as a result the corresponding plasmon is located at 3.29 eV, slightly below the Mie value of 3.4 eV.

The RPA oscillator-strength distribution of Na_{1982} is displayed in Fig. 4 of Ref. 5. For Na_{1982} , the matrix RPA yielded⁴ $\alpha_0 = 1.04$, and thus the plasmon is located at 3.33 eV, again slightly lower than the classical Mie value, but slightly higher than the plasmon for Na_{952} (recent unpublished results confirm these trends for clusters up to 5500 sodium atoms²⁹).

Taking into account Ref. 4, where matrix RPA results were presented for other sufficiently large, but smaller sizes (namely, Na_{92} , Na_{138} , Na_{154} , Na_{196} , Na_{254} , and Na_{338}), we can conclude that the RPA plasmon approaches smoothly from below the classical Drude-Mie value as the size increases, while the static polarizability approaches from above the classical value of unity. Nowhere in this extensive range of sizes have we found

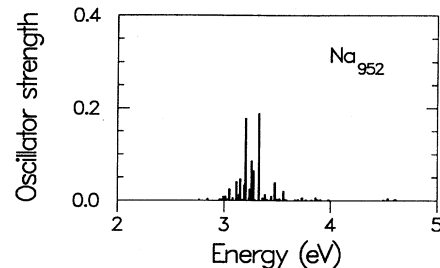


FIG. 1. Random-phase-approximation oscillator-strength distribution of the dipole mode in the case of the neutral Na_{952} cluster (see text for details).

any indication or signal that the RPA may be unreliable for large Na clusters, in contrast to the conclusion of Ref. 11, which, however, was based on a *nonconverged* CI calculation for the rather small Na_{20} .

B. The limit of highly charged cationic clusters

Cationic metal clusters, M_N^{z+} (where N is the number of atoms), are stable in their ground states only for moderate values of the ratio, $f = x^2/(Nv)$, of the square of the excess charge, x , over the total number of electrons, Nv , in the neutral cluster (v is the valency, which in the case of sodium equals unity). Above a certain critical value f_{cr} , they are unstable against spontaneous fission. In the case of sodium, a liquid-drop estimate³⁰ yields $f_{\text{cr}} = 0.39$, and as a result, the highly charged Na_{60}^{20+} is unstable.

Naturally, such highly unstable clusters have not attracted much attention. From a theoretical perspective concerning the optical response, however, they represent an interesting exact many-body limit, against which the different many-body approaches can be tested. This limit arises from the property that the electronic density is well confined within the boundary of the positive jellium background. In this instance, the confining potential generated by the positive background can be well approximated by its harmonic part (this situation is analogous to the case of parabolic confinement, familiar from the physics of quantum dots and semiconductor quantum wells^{16,17}). It is known that in such a case the center-of-mass motion of the electron gas separates exactly from the individual motions, irrespective of the nature of the two-body force.^{16,17} Consequently, the photoabsorption spectrum of a highly cationic cluster must consist of precisely one line having 100% of the oscillator strength. The frequency of this line coincides with the frequency of the confining parabolic potential (generalized Kohn theorem¹⁶).

In particular, the confining potential inside the uniform spherical jellium is equal to

$$U_J(r) = \text{const} + \frac{2\pi\rho}{3}r^2 = \text{const} + \frac{1}{2}m_e\omega_{\text{Mie}}^2r^2, \quad (1)$$

where ρ denotes the jellium density. We note that the frequency corresponding to the harmonic confinement coincides with the classical Mie frequency of a spherical metallic particle, namely, with $\omega_{\text{Mie}} = \omega_{\text{pla}}/\sqrt{3}$. As a result, the energy of the plasmon in the case of Na_{60}^{20+} must be practically equal to 3.4 eV.

To test this model-independent prediction, we have carried a matrix-RPA calculation for Na_{60}^{20+} , and have displayed the result in Fig. 2. Indeed, the RPA response of Na_{60}^{20+} consists of a single line having 99.975% of the total oscillator strength. The energy of this line is 3.412 eV, namely, it is located only 0.35% away from the Mie value, in very good agreement with the prediction of the Kohn theorem. We note that the calculated Thomas-Reiche-Kuhn (TRK) sum rule is only 0.025% below the theoretical value of 40 electrons.

Since this RPA result agrees with the exact many-body

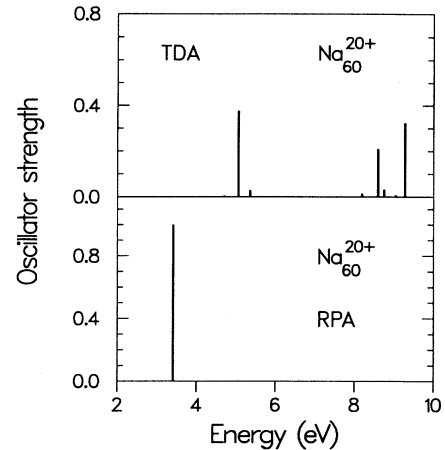


FIG. 2. Random-phase-approximation versus TDA oscillator-strength distribution of the dipole mode in the case of the highly charged cationic Na_{60}^{20+} cluster (see text for details).

prediction to a very high degree, it offers a stringent test of the accuracy and reliability of the method when applied to medium-size clusters. The matrix RPA results presented in the previous paragraph can be contrasted with the CI results for highly cationic sodium clusters. Due to computational restrictions, the authors of Ref. 11 have calculated the optical response of a series of smaller strongly ionized cations, namely, for Na_N^{z+} (in our notation) with $N - z = 8$. For $N = 28$ and $z = 20$, they found that, with respect to the excess charge, the CI results had fully converged to 3.79 eV. Since the Mie energy in their case is 3.49 eV (corresponding to an r_s of 3.93 a.u.), the CI result disagrees with the exact many-body prediction by $0.3/3.49=8.8\%$, a large discrepancy compared to the 0.35% of the matrix RPA. Reference 11 also reports that the calculated TRK sum rule for Na_{16}^{8+} was $0.109 \text{ nm}^2 \text{ eV}$, compared to a theoretical value of $0.088 \text{ nm}^2 \text{ eV}$, namely, there is a large overestimation by 24%, which compares unfavorably with the very small (only 0.025%) underestimation of the matrix-RPA calculation for Na_{60}^{20+} .

The RPA results presented in this subsection, and the comparison with corresponding CI results for Na_N^{z+} clusters, suggest that there is a strong correlation between plasmon position and the extent of satisfying the TRK sum rule. In this context, it is instructive to examine in detail how the position of the RPA plasmon converges to the exact result when the size of the basis set increases, and how this convergence in plasmon position correlates with the convergence of the energy weighted sum, $S(E1)$. For the case of Na_{60}^{20+} , Table I lists the successive plasmon positions, values of the $S(E1)$ sum, and static polarizabilities calculated with the matrix RPA as a function of the character $\Delta\mathcal{N}$ of particle-hole transitions included in the basis set [$\mathcal{N} = 2(n-1) + l$ denotes the principal quantum number of a single-particle level (n is the number of nodes minus one and l is the angular momentum of the single-particle state)]. When solely the $\Delta\mathcal{N} = 1$ transitions are included in the basis set, the TRK sum is exhausted already by 93.95%. How-

ever, the plasmon position is at 3.74 eV, or 10% above the exact value of 3.4 eV (this error is of comparable magnitude with the error of the CI calculations for highly ionized clusters with eight delocalized electrons). To reach the high quality RPA results presented in Fig. 2 (and discussed above), the RPA basis set needs to be enlarged in order to include the $\Delta\mathcal{N} = 7$ transitions. The basis-dependent RPA results in Table I show that satisfying the sum rule to high accuracy is a prerequisite for any calculation in yielding the correct plasmon position.³¹

Random-phase-approximation results for highly ionized clusters have not been presented earlier, since it is doubtful that such clusters can live long enough to be studied under experimentally controlled situations. However, they are helpful in the present context, since they show, that due to the agreement with the parabolic-confinement prediction, the RPA is closer to the exact many-body problem than a CI calculation in the best space. This in turn suggests that any CI simulation of RPA results requires an enlargement of the best space, rather than a restriction of it to smaller spaces, as was presumed in Ref. 11 in connection with the neutral Na_{20} .

C. The case of Na_{20}

Reference 11 suggested that a CI analog of the RPA plasmon for Na_{20} can be constructed by the following procedure, namely: (i) by considering a CI ground state which includes only $2p$ - $2h$ correlations, and (ii) by including only $1p$ - $1h$ and $3p$ - $3h$ pairs in the excited space. The CI plasmon in this limited subspace shares a double-line profile with the RPA-LDA plasmon of Ref. 1, a similarity that was used to support the claim that the CI prescription adopted in Ref. 11 produced indeed an RPA-like plasmon. However, it is erroneous to isolate the profile as the only characteristic feature of the RPA plasmon in Na_{20} . As important as the profile may be, the position of the resonance cannot be overlooked, when comparing CI analog and RPA plasmons. Indeed, the double-line profile of the RPA plasmon depends sensitively on its position, a property that was explained in Ref. 1(b) by approximating the RPA equations for Na_{20} by a simple two-level model. In particular, it was found that the dou-

TABLE I. The variations in RPA of plasmon position, energy weighted sum $S(E1)$, and static polarizability α_0 in the case of Na_{60}^{20+} as shells of higher $\Delta\mathcal{N}$ character are successively added to the particle-hole basis. A notation like $(\Delta\mathcal{N} =) 1 - 7$ denotes the minimum and maximum character of the shells considered at each step. The plasmon position is given in eV. The $S(E1)$ sum is expressed in units of $\hbar^2 e^2 / 2m_e$, and the static polarizability in units of R^3 . The numbers in parentheses express the relative value of $S(E1)$ with respect to the TRK sum-rule value of 40.

$\Delta\mathcal{N}$	Position	$S(E1)$	α_0
1	3.742	37.582 (93.95%)	0.82
1 - 3	3.460	39.788 (99.47%)	0.96
1 - 5	3.415	39.982 (99.95%)	0.99
1 - 7	3.412	39.990 (99.97%)	0.99

ble line was the result of an interaction between the plasmon and the $2s \rightarrow 3p$ particle-hole excitation, and that the splitting was effective only when the plasmon was situated ± 0.3 eV away from the location of the $2s \rightarrow 3p$ state (whose energy was 2.74 eV). Indeed, it was found that the plasmon before fragmentation was located at 2.8 eV, well within the required distance of 0.3 eV away from the $2s \rightarrow 3p$ excitation. The coupling between the plasmon and the $2s \rightarrow 3p$ transition finally yielded two lines, one at 2.6 eV and the other at 2.9 eV.

Let us examine now the location of the CI analog. According to Ref. 11 (see, Fig. 16, middle panel) the ‘‘RPA-like’’ plasmon comprises two lines, one at 3.6 eV and the other at 4.2 eV. They are both above the classical Mie value of 3.49 eV, in contrast with the experimentally¹² and theoretically¹³ established trend (namely, that the plasmon shifts below the Mie value as the cluster size decreases). These numbers (i.e., 3.6 and 4.2 eV) are so high in the energy scale that they alone, by themselves, reveal the falsity of associating the CI analog of Ref. 11 with the RPA plasmon. The appearance of a double-line profile in the CI analog is fortuitous and has the same origin as the multippeak profile of the Tamm-Dancoff approximation (TDA) (see Fig. 16, left panel).

Another apparent property that a CI solution must exhibit before being viewed as ‘‘RPA like’’ is the preservation of sum rules, a property well established^{18,19} in RPA theory. For the particular RPA calculation¹ for Na_{20} , the error in the TRK sum rule was only 0.52% below the theoretical value of 20 electrons. In the case of Na_{20} , Ref. 11 did not provide any information regarding sum rules. However, from an inspection of its Fig. 5 (where information was provided for the smaller sizes $N = 2 - 10$), one sees that already for $N = 10$ the CI calculation violates the TRK sum rule by 22%.

For the case of the CI calculation for Na_{20} , one can only surmise that the violation of the sum rules is even more pronounced. This can be seen by using the well known expression¹⁹ for the ratio, m_3/m_1 , of the third sum-rule moment over the first (TRK) sum-rule moment, namely,

$$E_3 = \sqrt{\frac{m_3}{m_1}} = \hbar\omega_{\text{Mie}} \left[1 - \frac{\Delta N_e}{N_e} \right]^{1/2}, \quad (2)$$

where N_e is the total number of delocalized valence electrons in the cluster and ΔN_e denotes the number of electrons outside the positive jellium background (the so-called spillout). It is known that the quantity E_3 provides an upper limit for the centroid of any strength distribution, and that this result is model independent. For the CI analog (see, middle panel of Fig. 16 in Ref. 11), an appropriate minimum value for E_3 is 3.8 eV (which is a compromise between the two peaks at 3.6 eV and 4.2 eV). Entering this value into Eq. (2) yields a value of $\Delta N_e = -3.57$ electrons for the spillout of Na_{20} . This negative value is certainly erroneous and indicates that the CI calculation violates the sum rules to an unacceptable degree; it also illustrates how the violation of the sum rules and the very high location of the CI plasmon lines are intertwined (this is true both for the so-called RPA-like subspace in the middle panel, as well as for the

best space in the right panel of Fig. 16).

We further remark that the absence of a double line in the best CI plasmon for Na_{20} (Fig. 16, right panel of Ref. 11) can be traced directly to its high position, since the single-particle spectra, and thus the resulting particle-hole transitions, used in both CI and RPA¹ calculations are similar. Namely, the CI calculation for Na_{20} used also an LDA potential to generate the single-particle states, precisely as is done in the matrix RPA. This LDA single-particle spectrum is listed in Table III of Ref. 11. An inspection of this table shows that the CI $2s$ state lies at -2.74 eV and that the $3p$ state lies at 0.14 eV, thus yielding a value of 2.88 eV for the $2s \rightarrow 3p$ transition entering into the CI calculation. As a result, the best CI plasmon at 3.6 eV (see, Fig. 16, right panel of Ref. 11) is located 0.72 eV away from the crucial $2s \rightarrow 3p$ transition, a separation which, according to the two-level analysis of Ref. 1(b), is far outside the required range (i.e., 0.3 eV) for the development of a double line through the interaction of the plasmon with this special transition.

We conclude that sufficient attraction (downward shift) is not generated by the CI spaces used in Ref. 11 in order to push the oscillator strength to lower energies and bring the CI plasmon in agreement with the RPA plasmon (as well as in agreement with the experiment). This lowering of the energy of the CI plasmon can only be achieved by an enlargement of the best space, a requirement that is beyond the available computational capacity at present. It is clear, however, that since lowering the energy of the CI plasmon is crucial in establishing similarity with the RPA, it is wrong to assume that ‘‘RPA-like’’ solutions can be produced by a restriction of the best CI space.

III. GROUND-STATE CORRELATIONS

We now turn our attention to the fundamental causes which guarantee that the matrix RPA satisfies all the consistency requirements as discussed in Sec. II.

A. The RPA ground state

Several publications^{21–27} have demonstrated that the RPA ground state comprises contributions of all $2np-2nh$ excitations of even order. Thus the claim¹¹ that an RPA-like analog can be extracted from the CI calculations when the latter are restricted to no higher than $2p-2h$ excitations for the ground state and up to $3p-3h$ excitations for the collective dipole excited state, must have been based on the assumption that, to a good approximation, the RPA ground state, $|\text{RPA}\rangle$, is described in all instances by its first two terms, and that higher terms can be omitted. Naturally, such an approximation may be valid in some instances (e.g., in the case of beta decay in heavy nuclei³²), but is wrong in the case of metal clusters. A property that Koskinen *et al.* overlooked in making analogies³³ with this specialized nuclear process is that beta decay is not a good case for assessing the importance of ground-state correlations in nuclei,

because this is a charge-exchange transition. In fact, it is known that for charge-exchange modes in heavy nuclei (namely, Isobaric analog states, Gamow-Teller states, etc.) RPA and TDA modes are quite close,^{34,35} because of Pauli blocking caused by neutron excess which reduces the backward-going Y amplitudes.³⁶

A comparison between TDA and RPA results provides an easy way to assess (at least qualitatively) the importance of higher-order terms in the RPA ground state of metal clusters. Figs. 2 and 3 display such a comparison for two different cases, namely, the highly ionized Na_{60}^{20+} and the neutral Na_8 . It is seen that TDA and RPA results are drastically different, which indicates that the RPA ground state in metal clusters cannot be truncated at the $2p-2h$ level and that strong higher-order correlations are present in the ground state of the system.

We note that the large difference between RPA and TDA response should not be construed as a warning that the RPA level of approximation is insufficient for describing the photoabsorption of metal clusters, and that consideration of *extensions*³⁷ of RPA is indispensable. Indeed this point is illustrated by the case of Na_{60}^{20+} (see Fig. 2) for which the exact many-body result is *a priori* known (see Sec. IIB). Namely, as seen from Fig. 2, the matrix RPA yields the correct answer despite the large difference with the TDA response. This, in its turn, suggests that for metal clusters the single-particle occupation probability distribution, N_i , associated with the correlated RPA ground state exhibits small or moderate deviations from the corresponding distribution, N_i^0 , associated with the uncorrelated TDA ground state (thus guaranteeing the validity of the quasiboson approximation), even though there is a large difference between these two ground states. In this respect, metal clusters represent systems with unique behavior, very different from the behavior of atomic nuclei.

Before proceeding further to offer explicit supporting evidence for the above suggestion, we need to clarify the

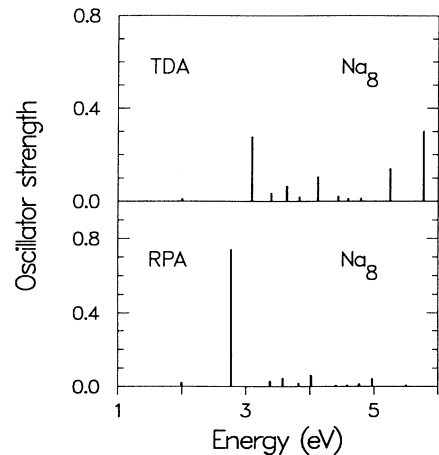


FIG. 3. Random-phase-approximation versus TDA oscillator-strength distribution of the dipole mode in the case of the neutral Na_8 cluster (see text for details).

use of the term correlations in the present paper, since many times in the nuclear literature this term has a double meaning referring both to the difference between the correlated and uncorrelated ground states and to the deviations of the corresponding single-particle occupation probability distributions. Unless explicitly noted, henceforth, the term should be construed as referring solely to the difference between the ground states.

To gain a deeper understanding of the nature of RPA correlations, we have addressed the question of the structure of $|\text{RPA}\rangle$ and have carried an explicit quantitative analysis of the contributions of the different $2np-2nh$ terms. To this end, we followed the formulation of Refs. 23 and 25, a brief outline of which is given below for the convenience of the reader.

We consider the case of spherical clusters, where it is convenient to introduce⁴ an angular-momentum-coupled creation operator, $A_{ph}^\dagger(L, M)$, constructed as a linear superposition of uncoupled particle-hole operators, $a_p^\dagger a_h$, having angular momenta l_p and l_h , namely,

$$A_{ph}^\dagger(L, M) = \frac{1}{\sqrt{2}} \sum_{m_p, m_h, \sigma} (l_p, l_h, m_p, m_h | LM) (-)^{l_h + m_h} \times a_{l_p, m_p, \sigma}^\dagger a_{l_h, -m_h, \sigma}, \quad (3)$$

where the index σ denotes the spin variable. The expression in parenthesis is the usual Clebsch-Gordan coefficient expressing the coupling of two angular momenta (l_1, l_2) with projections (m_1, m_2) to a total angular momentum L with total projection M .

If the uncorrelated ground state is denoted by $|0\rangle$, the RPA ground state has the following *exponential* form:^{23,25}

$$|\text{RPA}\rangle = \mathcal{N}_0 \exp \left\{ -\frac{1}{2} \sum_{L, M} \sum_{p, h, p', h'} (-)^{L-M} C_{php'h'}^L \times A_{ph}^\dagger(L, M) A_{p'h'}^\dagger(L, -M) \right\} |0\rangle. \quad (4)$$

The exponential form of Eq. (4) results from the requirement that the RPA ground state is the vacuum of all RPA excitations, together with the use of the quasiboson approximation. This latter approximation is defined as

$$[a_{l_h, m_h, \sigma}^\dagger a_{l_p, m_p, \sigma}, a_{l_p', m_p', \sigma'}^\dagger a_{l_h', m_h', \sigma'}] \approx \delta_{l_p, l_p'} \delta_{m_p, m_p'} \delta_{l_h, l_h'} \delta_{m_h, m_h'} \delta_{\sigma\sigma'}, \quad (5)$$

in the uncoupled particle-hole representation and as

$$[A_{ph}(L, M), A_{p'h'}^\dagger(L', M')] \approx \delta_{pp'} \delta_{hh'} \delta_{LL'} \delta_{MM'}, \quad (6)$$

in the coupled particle-hole representation.

The correlation coefficients $C_{php'h'}^L$ determine the amplitudes for the presence of two, four, six, ..., $2n$ particle-hole pairs in the RPA ground state. From the vacuum property of the RPA ground state and the quasiboson

commutators, it follows that the correlation coefficients are solutions of the set of equations,^{23,25}

$$\sum_{p, h} X_{ph}^\nu(L) C_{php'h'}^L = Y_{p'h'}^\nu(L) \quad \text{for all } p', h', \nu, L, \quad (7)$$

where the X and Y amplitudes are the eigenvectors of the RPA secular problem.^{4,7}

The probability P_{2n} to find $2np-2nh$ excitations in the ground state is given by the n th term in the expansion of the scalar product $\langle \text{RPA} | \text{RPA} \rangle$, i.e., by

$$P_{2n} = \mathcal{N}_0^2 \frac{1}{n!} \left(\frac{u^2}{2} \right)^n, \quad (8)$$

where

$$\mathcal{N}_0^2 = \exp(-u^2/2), \quad (9)$$

and

$$u^2 = \sum_L \sum_{p, h, p', h'} (2L+1) (C_{php'h'}^L)^2. \quad (10)$$

The probability for finding the uncorrelated ground state, $|0\rangle$, in the correlated $|\text{RPA}\rangle$ is

$$P_0 = \mathcal{N}_0^2, \quad (11)$$

while the average number of excited particles in the RPA ground state is given by

$$\bar{n} = \sum_{n=1}^{\infty} 2nP_{2n} = u^2. \quad (12)$$

The final quantities, which we are interested in calculating, are the occupation number N_p and the depletion number $1 - N_h$ for a single particle or hole state,²⁶ respectively, i.e.,

$$N_p = \langle \text{RPA} | a_{l_p, m_p, \sigma}^\dagger a_{l_p, m_p, \sigma} | \text{RPA} \rangle = \frac{1}{2} \frac{1}{2(2l_p+1)} u_p^2, \quad (13)$$

and

$$1 - N_h = \langle \text{RPA} | a_{l_h, m_h, \sigma} a_{l_h, m_h, \sigma}^\dagger | \text{RPA} \rangle = \frac{1}{2} \frac{1}{2(2l_h+1)} u_h^2, \quad (14)$$

where

$$u_p^2 = \sum_{L, \nu, h} (2L+1) (Y_{ph}^\nu)^2, \quad (15)$$

and

$$u_h^2 = \sum_{L, \nu, p} (2L+1) (Y_{ph}^\nu)^2. \quad (16)$$

The values N_p and $1 - N_h$ must be sufficiently smaller than unity in order for the quasiboson approximation (and, thus, the RPA) to be valid, since

$$\begin{aligned} \langle \text{RPA} | [A_{ph}(L, M), A_{p'h'}^\dagger(L, M)] | \text{RPA} \rangle \\ = \delta_{pp'} \delta_{hh'} (N_h - N_p). \end{aligned} \quad (17)$$

We note that — due to the spherical-shell degeneracy factors, $1/(2l+1)$, in Eqs. (13) and (14) — small values of N_p and $1 - N_h$ do not necessarily imply a small *absolute* value for the average number of excited particles $\bar{n} = u^2$ [see, Eqs. (12) and (10)], which controls the distribution of the $2np-2nh$ components in the RPA ground state through the Poisson³⁸ distribution (8) (however, small values of N_p and $1 - N_h$ do imply a small *relative* value of \bar{n} with respect to the total number N_e of delocalized valence electrons, i.e., $\bar{n}/N_e \ll 1$). A characteristic feature of a Poisson distribution is the presence, in each one of its members, of the exponential factor $\exp(-u^2/2)$, which can cause a rapid suppression of the weight of the uncorrelated ground state $|0\rangle$ [see, Eqs. (9) and (11)]. As we will explicitly discuss below, a situation arises in metal clusters where the uncorrelated ground state $|0\rangle$ has small overlap with the RPA ground state,

$$\langle 0 | \text{RPA} \rangle \approx 0, \quad (18)$$

but still gives good results for single-particle occupation numbers,

$$\langle 0 | a^\dagger a | 0 \rangle \approx \langle \text{RPA} | a^\dagger a | \text{RPA} \rangle. \quad (19)$$

We have calculated³⁹ the occupation numbers N_p and the depletion numbers $1 - N_h$, the average number \bar{n} , and the probabilities P_{2n} for the four clusters Na_{20} , Na_{21}^+ , Na_{41}^+ , and Na_{441}^+ , and have displayed the results in Fig. 4, Table II, and Fig. 5, respectively.

From Fig. 4, one sees that in all four cases the quantities N_p and $1 - N_h$ are indeed small, none of them being larger than 0.10. On the other hand (see Table II), the average number, \bar{n} , of excited particles is larger than unity in all four cases and exhibits a rather rapid increase in absolute value with increasing cluster size. In particular, for Na_{441}^+ , one has $\bar{n} = 30.0$, which yields a vanishingly small weight for the $0p-0h$ contribution, namely, $\mathcal{N}_0^2 = \exp(-15.0) \approx 3.06 \cdot 10^{-7}$. We note that the average number of excited particles above the Fermi level is small in relative terms and never exceeds 10%.

Figure 5 explicitly demonstrates that truncating the $2np-2nh$ exponential series of $|\text{RPA}\rangle$ at the $2p-2h$ level is a bad approximation in all three cases, since higher P_{2n} probabilities remain considerably large. Specifically, for Na_{21}^+ the ratio $P_4/P_2 \approx 0.5$, while $P_0 \approx P_2 \approx 0.4$ (the P_{2n} probability distribution for the neutral Na_{20} is practically indistinguishable from that of the isoelectronic singly charged Na_{21}^+). The large RPA suppression of P_0 is a crucial element for appreciating the weakness of the CI method. Indeed, even for the *best* space, the weight, P_0^{CI} , of the $0p-0h$ configuration in the CI ground state for Na_{20} is 69%,¹¹ which is much larger than the 40% of the RPA calculation in the case of Na_{21}^+ (or Na_{20}). This disparity between CI and RPA indicates again how far away the CI calculation is from being RPA like. Naturally, only an enlargement, and not a restriction, of the *best* space can further reduce P_0^{CI} and bring it closer to the RPA standard.

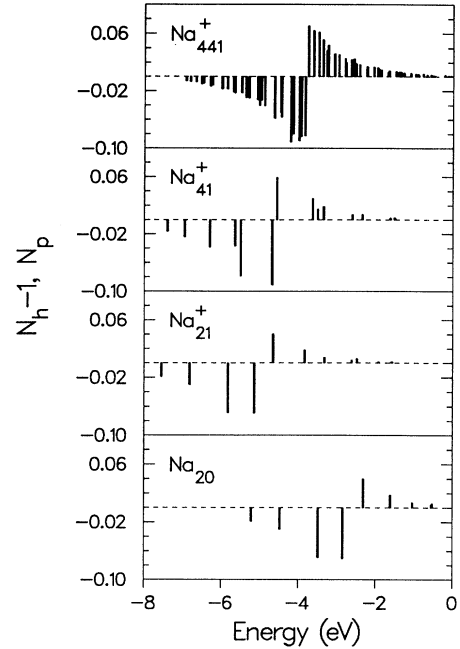


FIG. 4. Occupation numbers $N_p > 0$ for particle states and the opposite of depletion numbers $N_h - 1 < 0$ for hole states in the RPA ground state [see Eqs. (13) and (14)] for the four clusters Na_{20} , Na_{21}^+ , Na_{41}^+ , and Na_{441}^+ . The x axis denotes the energy of the hole or particle states. Plotting the opposite of depletion numbers allows for an easier visualization of the Fermi energy.

For Na_{41}^+ , the RPA P_0 is only 0.15, and even the $8p-8h$ component has 8% probability (see Fig. 5). In the case of Na_{441}^+ , the RPA P_{2n} curve resembles a Gaussian distribution⁴⁰ centered around $2n = 30 \approx \bar{n}$. In this case, we note the vanishingly small weight for the first five terms in the exponential expansion of $|\text{RPA}\rangle$.

The similarity in the ground-state correlations, as well as in the single-particle occupation probabilities, between the isoelectronic clusters Na_{20} and Na_{21}^+ is particularly interesting, since the profiles of their photoabsorption spectra are quite dissimilar. Indeed it has been found that the neutral Na_{20} exhibits a double peak^{1,3,4}, while the singly-charged Na_{21}^+ is characterized by a single absorption band. This implies that the details of the photoabsorption profiles do not influence the ground-state correlations or the extent of validity of the quasiboson approximation. *Vice versa*, ground-state correlations influence directly only the position of the plasmon. The various photoabsorption profiles in isoelectronic cluster sequences are the direct result, not of variations in ground-state correlations, but of variations in the single-particle

TABLE II. The average number \bar{n} [Eq. (12)] and the percentage of excited particles above the Fermi level in the RPA ground state.

	Na_{20}	Na_{21}^+	Na_{41}^+	Na_{441}^+
\bar{n}	1.82	1.81	3.84	30.04
%	9.10	9.05	9.60	6.83

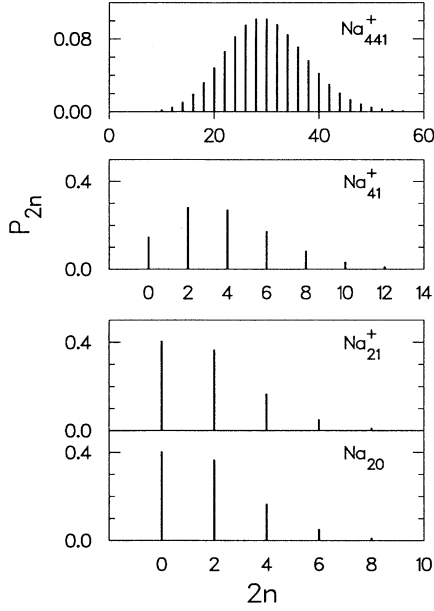


FIG. 5. The probability distribution P_{2n} for finding a $2np-2nh$ configuration in the RPA ground state [see Eq. (8)] of Na_{20} , Na_{21}^+ , Na_{41}^+ , and Na_{441}^+ . The uncorrelated ground state (reference determinant) corresponds to $2n = 0$.

spectra (due to the excess charge) and of the ensuing variations in the interplay of the particle-hole transitions with the plasmon (see, Refs. 1, 3, 4 for a detailed discussion of this effect).

The explicit quantitative analysis in this subsection has shown that the linear response of metal clusters is characterized by the presence of strong correlations (namely, a large difference between correlated and uncorrelated ground states) together with small or moderate deviations between the corresponding single-particle occupation probability distributions. This behavior becomes more accentuated the larger the size of the cluster. What happens can be explained in a qualitative way as follows: Let us assume that we have a sodium cluster Na_N with $N = 10\,000$ atoms, and let us suppose that 1% of the delocalized valence electrons are on the average above the Fermi level in the ground-state wave function. This yields $\bar{n} = 100$, which means that the P_{2n} distribution will be a Gaussian centered at $2n = 100$, namely, the most important contribution in the correlated ground state will arise from the $100p-100h$ excitations. Now a $100p-100h$ excitation seems to be separated by a large difference from the $0p-0h$ initial determinant (it is customary to think that only a $2p-2h$ state is close in some vague sense to the initial $0p-0h$ determinant). However, the validity of the quasiboson approximation does not rest on the proximity or not of states, but on the proximity of single-particle occupation probabilities. Namely, in the example considered here only 100 occupation numbers can be influenced out of 10 000. Since there are many ways (permutations) of choosing 100 electrons out of 10 000, the two occupation-number distributions are very close, even though the two ground states are rather apart as wave functions [see also Eqs. (18) and (19)].

B. Physical reasons for the strong higher-order correlations

In this subsection, we provide an explanation why the RPA yields such strongly correlated ground states in the case of metallic clusters. Specifically, we will show that this behavior is related to the long-range character of the Coulomb force, which in this respect is dissimilar from the short-range character of the nuclear forces.

A main consequence of the long-range character of the Coulomb force is that the plasmon energy, as a function of size, increases and slowly approaches a finite value, namely, the classical Mie energy [on the contrary, the energy of the nuclear giant dipole excitation decreases as $A^{-1/3}$ as a function of size (A is the nuclear mass number)]. The finite value of the Mie energy results in large values for the backward-going RPA Y amplitudes (large in relative terms with respect to the forward-going X amplitudes), and thus in exceptionally strong correlations in the RPA ground state. This can be seen as follows.

Let us focus on the dipole mode ($L = 1$) and let us assume for simplicity that the RPA produces one single collective excitation (plasmon), $|c\rangle$, with energy $\hbar\omega_c$ [this assumption is better fulfilled for large and highly cationic clusters (see Secs. II A and II B)]. Using a separable-force approximation for the Coulomb force,⁵ an approximation that is valid for large metal clusters, the RPA amplitudes are given⁵ by an analytic expression⁴¹ as follows,

$$\begin{aligned} X_{ph}^c &= C \frac{\langle p || \mathcal{M}(E1) || h \rangle}{\hbar\omega_c - \varepsilon_{ph}}, \\ Y_{ph}^c &= C \frac{\langle p || \mathcal{M}(E1) || h \rangle}{\hbar\omega_c + \varepsilon_{ph}}, \end{aligned} \quad (20)$$

where the particle-hole transitions have energies $\varepsilon_{ph} = \varepsilon_p - \varepsilon_h$, and $\langle p || \mathcal{M}(E1) || h \rangle$ is the reduced matrix element⁴ between single-particle states of the electric dipole operator $\mathcal{M}(E1; \mu) = \sqrt{4\pi/3} \, er Y_{1\mu}(\hat{\mathbf{r}})$, $Y_{1\mu}(\hat{\mathbf{r}})$ being the corresponding spherical harmonic. C is a normalization constant.

From Eq. (20), one finds that the diagonal ratios Y_{ph}^c/X_{ph}^c are given by

$$\frac{Y_{ph}^c}{X_{ph}^c} = \frac{\hbar\omega_c - \varepsilon_{ph}}{\hbar\omega_c + \varepsilon_{ph}}. \quad (21)$$

The particle-hole transitions which mainly contribute to the TRK sum-rule are those with $\Delta\mathcal{N} = 1$ or 3 .^{4,5} The energy of these particle-hole transitions varies roughly as $N^{-1/3}$ and thus becomes smaller the larger the size of the cluster.^{4,5} Since the plasmon energy $\hbar\omega_c$ in the right-hand side of Eq. (21) remains finite in value as the size increases (it approaches the classical Mie value), it follows from Eq. (21) that the relevant ratios Y_{ph}^c/X_{ph}^c (i.e., those associated with the $\Delta\mathcal{N} = 1$ or 3 transitions) increase steadily and approach unity for very large clusters. Indeed, our numerical calculations provide a confirmation of this trend. Specifically, the largest Y_{ph}^c/X_{ph}^c ratios⁴² are 0.30 for Na_8 , 0.57 for Na_{60}^{20+} , 0.73 for Na_{338} , 0.81 for Na_{952} , and 0.85 for Na_{1982} .

We have addressed the behavior of the diagonal ratios Y_{ph}^c/X_{ph}^c , because they determine the magnitude of the correlation coefficients $C_{php'h'}^L$, as can be seen from Eq. (7), and thus the precise contribution of higher-order correlations in the RPA ground state. In the case of clusters, we have shown that these ratios have large values (approaching unity for large clusters) as a result of the long-range character of the repulsive Coulomb force. This behavior provides the underlying physical reason for the presence of the strong higher-order correlations calculated in Sec. III A, which became stronger the larger the size of the cluster.

The backward-going amplitudes represent the influence of ground-state correlations on the different quantities associated with the collective modes (e.g., plasmon position, etc.). In particular, besides generating through Eq. (7) the strong higher-order components in the ground state, the large diagonal ratios Y_{ph}^c/X_{ph}^c are instrumental in quenching (with respect to the TDA or the unperturbed case) the RPA dipole transition probabilities, $B(E1; \nu)$, associated with the RPA states (we consider all RPA states ν here), thus creating the conditions for the preservation of the TRK sum rule. This quenching is remarkably efficient, since our calculations show that the energy weighted sum, $S(E1)$, for the TDA calculation of Na_{60}^{20+} is 244.89 to be contrasted with the TRK sum-rule value of 40. Thus TDA violates the TRK sum rule by 612%, while the corresponding RPA result deviates from the theoretical value only by 0.025%. It is interesting to demonstrate what happens in detail, and thus we repeat here the RPA expression for $B(E1; \nu)$, namely,

$$B(E1; \nu) = \frac{2}{3} \sum_{p,h} |\langle p || \mathcal{M}(E1) || h \rangle (X_{ph}^\nu - Y_{ph}^\nu)|^2. \quad (22)$$

The energy weighted sum is then given by the expression

$$S(E1) = \sum_{\nu} E_{\nu} B(E1; \nu), \quad (23)$$

where the energies E_{ν} are the solutions of the RPA secular equation. In the case of TDA, corresponding expressions result by formally setting $Y_{ph}^\nu = 0$ in Eqs. (22) and (23). From Eqs. (22) and (23), it is seen that the large ratios Y_{ph}^ν/X_{ph}^ν provide the strong quenching of $B(E1; \nu)$ and $S(E1)$ by acting through the differences $(X_{ph}^\nu - Y_{ph}^\nu)$.⁴³

We further mention that the behavior of the RPA backward-going amplitudes in metal clusters is quite dissimilar from the case of nuclear giant dipole excitations whose energy goes to zero for large mass numbers due to

the short-range character of nuclear forces. As pointed out in Ref. 7, the larger ratios Y_{ph}^c/X_{ph}^c in metal clusters as compared to the case of nuclei is the origin of the very different importance of anharmonicities in the two cases. The two-plasmon spectrum⁷ in Na_{20} is highly anharmonic. On the contrary, in the nuclear case,⁴⁴ the two-boson spectrum associated with the double excitation of the giant dipole resonance is almost harmonic.

IV. CONCLUSIONS

We conclude that keeping only the first two terms in the exponential expansion of the RPA ground state is a poor approximation in the case of metal clusters. To simulate the RPA solutions, one needs to enlarge the *best* CI space, rather than restrict it.

The discrepancies between the CI and RPA calculations result from numerical weaknesses of the former, since the lack of convergence prevents the CI method from developing in the ground state the Poisson-like distributed correlations (see Fig. 5), which are the hallmark of the RPA ground states in metallic clusters (these correlations are intricately related to the preservation of the TRK sum rule). The underlying physical reason for these strong higher-order correlations is the long-range character of the Coulomb interaction. In contrast to the CI method, the RPA [through the backward-going Y amplitudes, see Eq. (7)] possesses an efficient way of accounting for the strong higher-order correlations present in metal clusters. It is this ability, together with the validity of the quasiboson approximation due to small deviations of RPA single-particle occupation probabilities from those associated with the reference determinant, that makes the RPA such a powerful tool in describing the plasmon modes in clusters. In particular, the reliability of the RPA was demonstrated in two special model-independent cases, namely, the case of highly ionized (see Sec. II B) and the case of very large clusters (see Sec. II A).

ACKNOWLEDGMENTS

This research was partially supported by the U.S. Department of Energy (C.Y.), Grant No. FG05-86ER45234, and by the European Community within the program "Human Capital and Mobility," Contract No. CHRX-CT92-0075. One of the authors (F.C.) gratefully acknowledges the hospitality and financial support from the Division de Physique Théorique, IPN, Orsay, where part of this work was carried out.

¹ (a) C. Yannouleas, R.A. Broglia, and M. Brack, Phys. Rev. Lett. **63**, 255 (1989); (b) C. Yannouleas and R.A. Broglia, Phys. Rev. A **44**, 5793 (1991).

² C. Yannouleas, J.M. Pacheco, and R.A. Broglia, Phys. Rev. B **41**, 6088 (1990); C. Yannouleas and R.A. Broglia, Eu-

rophys. Lett. **15**, 843 (1991); C. Yannouleas, P. Jena, and S.N. Khanna, Phys. Rev. B **46**, 9751 (1992).

³ C. Yannouleas, Chem. Phys. Lett. **193**, 587 (1992).

⁴ C. Yannouleas, E. Vigezzi, and R.A. Broglia, Phys. Rev. B **47**, 9849 (1993).

- ⁵ C. Yannouleas and R.A. Broglia, *Ann. Phys. (N.Y.)* **217**, 105 (1992).
- ⁶ Ll. Serra, J. Navarro, M. Barranco, and N. Van Giai, *Phys. Rev. Lett.* **67**, 2311 (1991).
- ⁷ F. Catara, Ph. Chomaz, and N. Van Giai, *Phys. Rev. B* **48**, 18 207 (1993).
- ⁸ W. Ekardt, *Phys. Rev. B* **31**, 6360 (1985); J.M. Pacheco and W. Ekardt, *Ann. Phys. (Leipzig)* **1**, 254 (1992).
- ⁹ D.E. Beck, *Phys. Rev. B* **43**, 7301 (1991).
- ¹⁰ A. Rubio, L.C. Balbás, and J.A. Alonso, *Phys. Rev. B* **45**, 13 657 (1992).
- ¹¹ M. Koskinen, M. Manninen, and P.O. Lipas, *Phys. Rev. B* **49**, 8418 (1994).
- ¹² W.A. de Heer, *Rev. Mod. Phys.* **65**, 611 (1993).
- ¹³ V. Kresin, *Phys. Rep.* **220**, 1 (1992).
- ¹⁴ G. Mie, *Ann. Phys. (Leipzig)* **25**, 377 (1908).
- ¹⁵ C. Bréchnignac, Ph. Cahuzac, J. Leygnier, and A. Sarfati, *Phys. Rev. Lett.* **70**, 2036 (1993).
- ¹⁶ L. Brey, N.F. Johnson, and B.I. Halperin, *Phys. Rev. B* **40**, 10 647 (1989); J. Dempsey and B.I. Halperin, *ibid.* **47**, 4662 (1993).
- ¹⁷ P.A. Maksym and T. Chakraborty, *Phys. Rev. Lett.* **65**, 108 (1990).
- ¹⁸ M. Brack, *Phys. Rev. B* **39**, 3533 (1989).
- ¹⁹ M. Brack, *Rev. Mod. Phys.* **65**, 677 (1993).
- ²⁰ Equation (B1) in Ref. 19, which defines the RPA ground state as comprising solely $2p$ - $2h$ correlations, is in apparent error. Indeed, such a restricted definition is incompatible (Refs. 22 and 27) with the RPA quasiboson approximation.
- ²¹ R.A. Sorensen, *Nucl. Phys.* **25**, 674 (1961).
- ²² G.E. Brown and G. Jacob, *Nucl. Phys.* **42**, 177 (1963).
- ²³ E.A. Sanderson, *Phys. Lett.* **19**, 141 (1965).
- ²⁴ J. Da Providência, *Phys. Lett.* **21**, 668 (1966).
- ²⁵ D. Agassi, V. Gillet, and A. Lumbroso, *Nucl. Phys. A* **130**, 129 (1969).
- ²⁶ D.J. Rowe, *Nuclear Collective Motion* (Methuen, London, 1970), Chaps. 14.10, 13.1.
- ²⁷ P. Ring and P. Schuck, *The Nuclear Many-Body Problem* (Springer-Verlag, Heidelberg, 1980), Chap. 8.4.6.
- ²⁸ Ll. Serra, G.B. Bachelet, N. Van Giai, and E. Lipparini, *Phys. Rev. B* **48**, 14 708 (1993).
- ²⁹ F. Catara, Ph. Chomaz, and N. Van Giai (unpublished).
- ³⁰ W.A. Saunders, *Phys. Rev. A* **46**, 7028 (1992).
- ³¹ Similar convergence behavior has also been found in the case of RPA calculations for neutral clusters. For a description of the convergence of the $S(E1)$ sum as a function of the RPA basis set in the case of the neutral Na_8 , Na_{20} , and Na_{40} clusters, see Table II of Ref. 1(b). For a description of the convergence of the position of the plasmon as a function of the RPA basis set in the case of the neutral Na_8 , see Fig. 6 of Ref. 1(b).
- ³² L. Zhao and B.A. Brown, *Phys. Rev. C* **47**, 2641 (1993).
- ³³ P.O. Lipas (private communication).
- ³⁴ O. Civitarese, H. Müther, L.D. Skouras, and A. Faessler, *J. Phys. G* **17**, 1363 (1991).
- ³⁵ B. Lauritzen, *Nucl. Phys. A* **489**, 237 (1988).
- ³⁶ N. Van Giai and H. Sagawa, *Phys. Lett. B* **106**, 379 (1981).
- ³⁷ Several extensions of RPA (which go beyond the level of mean-field approximation) have been proposed in the nuclear-physics literature. Generally, they fall into two groups, namely, (i) those which aim at improving the quasiboson approximation and (ii) those which extend the definition of the RPA excitation operators to include $2p$ - $2h$ (and higher components). Among the former group, we mention the *renormalized* RPA [see D.J. Rowe, *Rev. Mod. Phys.* **40**, 153 (1968); F. Catara *et al.*, *Nucl. Phys. A* **579**, 1 (1994)] and the *self-consistent* RPA [see D. Janssen and P. Schuck, *Z. Phys. A* **339**, 43 (1991)]. It is not clear whether these extensions preserve the TRK sum rule. From the latter group, we mention the *second* RPA [see C. Yannouleas *et al.*, *Nucl. Phys. A* **397**, 239 (1983)]. This last extension explicitly preserves the TRK sum rule [see C. Yannouleas, *Phys. Rev. C* **35**, 1159 (1987)]. Although an object of legitimate future research, application of such extensions to metal clusters is beyond the scope of the present paper. In any case, because of favorable conditions for the validity of the quasiboson approximation and the close agreement between RPA results and experiment, we anticipate that only small corrections will be found as a result of consideration of such extensions.
- ³⁸ Ph.R. Wallace, *Mathematical Analysis of Physical Problems* (Dover, New York, 1984).
- ³⁹ In the calculation, we have included all excited RPA states with $L \leq 8$.
- ⁴⁰ For details of why a Poisson distribution approaches the profile of a sharply peaked and narrow Gaussian distribution when \bar{n} is large, see Ref. 38.
- ⁴¹ There is a difference in sign between the Y_{ph}^c as defined here and in Ref. 5. This is because Ref. 5 used the uncoupled particle-hole representation. In the present paper, we have preferred to use the coupled particle-hole representation, which is the one utilized in the actual numerical calculations.
- ⁴² See Figs. 6 and 7 of Ref. 4 and Table I of Ref. 1(b) for a detailed presentation of the X_{ph}^c and Y_{ph}^c amplitudes for Na_8 , Na_{338} , and Na_{20} , respectively.
- ⁴³ For the subtraction to be effective, the amplitudes X_{ph}^ν and Y_{ph}^ν must have the same sign. For large clusters, this is certainly true for all the particle-hole excitations of $\Delta\mathcal{N} = 1$ and 3 character. Even for the smallest clusters (see Ref. 42), this holds true for the particle-hole excitations of $\Delta\mathcal{N} = 1$ character.
- ⁴⁴ F. Catara, Ph. Chomaz, and N. Van Giai, *Phys. Lett. B* **233**, 6 (1989).